



## Chemical Modification of Montmorillonite K10 and Its Catalytic Activity

SERLY JOLANDA SEKEWAE<sup>1,\*</sup>, KARNA WIJAYA<sup>2</sup> and TRIYONO<sup>2</sup>

<sup>1</sup>Department of Chemistry, Faculty of Mathematics and Natural Sciences, Pattimura University, Ambon, Indonesia

<sup>2</sup>Department of Chemistry, Faculty of Mathematics and Natural Sciences, Gadjah Mada University, Yogyakarta, Indonesia

\*Corresponding author: E-mail: [sjsekewael@yahoo.com](mailto:sjsekewael@yahoo.com)

Received: 27 May 2019;

Accepted: 16 November 2019;

Published online: 31 January 2020;

AJC-19775

Montmorillonite K10 (Mt-K10) was chemically modified using a silica-zirconia mixture and the resulting product was named SZMK. The product had an increased total surface acidity, catalytic activity, porosity, and thermal stability. Ammonia adsorption tests and further verification with FTIR and TGA/DTA showed that the acidity of SZMK was higher (0.16 mmol/g) than that of Mt-K10. Catalytic performance was analyzed on the esterification reaction of lauric acid. Refluxing lauric acid and methanol (molar ratio of 1:20) for 20 h with a 20 % (w/w) catalyst showed that catalytic activity of SZMK is high, *i.e.* methyl laurate production 98.18% (w/w) was achieved.

**Keywords:** Acidity, Catalytic activity, Montmorillonite K10, Silica, Zirconia.

### INTRODUCTION

In previous years, numerous catalysts and catalytic processes have been developed and studied. However, many opportunities are available for development of new catalytic materials and processes. One challenge that can be focussed on is developing a solid acid catalyst that can be a mixed oxide montmorillonite clay nanocomposite. Nanocomposite clays with colloidal particles, for example, SiO<sub>2</sub>-Fe<sub>2</sub>O<sub>3</sub> [1,2], SiO<sub>2</sub>-ZrO<sub>2</sub> [3-5], SiO<sub>2</sub>-TiO<sub>2</sub> [6] and SiO<sub>2</sub>-Al<sub>2</sub>O<sub>3</sub> [7] have been developed. Generally, montmorillonite modification leads to high specific surface area, controllable pore size and thermally stable pillared clay.

Several researchers have used montmorillonite K10 (Mt-K10) and its modified compound as a solid acid catalyst in different organic reactions [2,8-10]. Catalysts are ecofriendly, non-corrosive, effectively work at intermediate temperatures and can replace conventional acid catalysts for converting reactants into a number of products.

In our earlier study, we proposed a novel method for synthesizing a solid acid catalyst [4]. We investigated how microwave radiation affects the synthesis and physico-chemical characteristics of silica-zirconia Mt-K10 nanocomposite [4]. For preparing the catalyst, silica-zirconia sol was intercalated into the

interlayer of montmorillonite clay and then calcinated using microwave irradiation [4].

In this study, montmorillonite K10 (Mt-K10) was chemically modified using mixed silica-zirconia and the parent products were compared with the final product for acidity, porosity, catalytic activity and thermal properties. Using EDX, their chemical properties were identified. Furthermore, by using ammonia-gravimetric and TGA/DTA analysis, FTIR and XRD, their acidity and thermal stability were studied. Additionally, porosity and catalytic activity were studied using N<sub>2</sub> gas adsorption and lauric acid esterification, respectively.

### EXPERIMENTAL

Montmorillonite K10 (Mt-K10) was obtained from Fluka (Chemica), tetraethyl orthosilicate (TEOS), ZrOCl<sub>2</sub>·8H<sub>2</sub>O, ethanol, NaOH, ammonium vapor, lauric acid, methanol and *n*-hexane were used as received.

X-ray diffraction patterns of the catalyst were recorded on the XRD-6000 Shimadzu. N<sub>2</sub> adsorption-desorption isotherms were measured at liquid nitrogen temperature with a gas sorption analyzer (Quantachrome, NOVA 11000). FTIR spectra were performed on a PC 8201 infrared spectrophotometer (Shimadzu Corporation, Japan). TGA/DTA curves were recorded on the Perkin Elmer TG/DTA EN 55011.

**General preparation of silica-zirconia/Mt-K10:** With the reported procedures, silica-zirconia/Mt-K10 was synthesized and characterised [4]. First, sol silica was prepared by mixing 41.6 g tetraethyl orthosilicate (TEOS), 10 mL HCl (2 M) and 12 mL ethanol for 2 h at room temperature. Subsequently, sol silica was mixed with 0.2 mol/L  $ZrOCl_2 \cdot 8H_2O$  at a molar ratio of Si:Zr of 10:1. The pH of the mixture was maintained at approximately 1.5 through titration with 0.2 mol/L NaOH. The solution was allowed to stand at room temperature for 1 h and then mixed with Mt-K10 at 1% w/v ( $CEC = 4.36 \times 10^{-4}$  meq/g) at a molar ratio Si:Zr:CEC = 50:5:1. The mixture was stirred for 20 h at room temperature. The product was centrifuged and washed with ethanol:water 1:1 volume ratio and then dried at room temperature. The dried sample was microwaved at 700 W power. The product had catalytic properties and was named SZMK.

**Characterization of acidity, porosity and thermal stability of catalysts:** The total surface acidity of solid catalysts was determined by allowing ammonium adsorption followed by FTIR measurements. The sample was placed in a desiccator and evacuated using a vacuum pump for 1 h before ammonium vapour exposure for 24 h. Then, the sample was reevacuated for 1 h at room temperature and analyzed using a PC 8201 infrared spectrophotometer. Furthermore, using the gravimetric method along with DTA/TGA analysis, total acidity of the samples was measured.

The sample porosity was determined using  $N_2$  gas sorption analyzer. Before measurement, samples were degassed at 300 °C for 3 h under reduced atmosphere. Furthermore, all samples were cooled with liquid nitrogen, leading to the formation of a single layer of nitrogen molecules on their surface. The specific surface area, average pore volume, average pore radius and pore size distribution were determined.

The thermal stability of samples was studied from 300-500 °C and further analyzed by using X-ray diffraction (XRD-6000 Shimadzu).

**Catalyst activity:** The catalyst was first used in lauric acid esterification at 20 % (w/w) dosage for refluxing of methanol and acid mixed in a molar ratio of 20:1 for 12 h. Then, the final mixture was analyzed using gas chromatography (GC) with an FID. The catalyst was reused for two cycles of the same reaction.

## RESULTS AND DISCUSSION

**Formation of silica-zirconia/Mt-K10:** In this study, initially, nanosol  $SiO_2$  particles were prepared through the hydrolysis of TEOS. Subsequently, zirconyl chloride octahydrate ( $ZrOCl_2 \cdot 8H_2O$ ) solution was added to nanosol  $SiO_2$ . Positively charged tetrameric ions  $[Zr_4(OH)_{14}(OH_2)_{10}]^{2+}$  was adsorbed on the negatively charged  $SiO_2$ , such that the linkage formed (Zr-O-Si) was accompanied by a bond dissociation (Zr-O-Zr) in the Mt-K10 framework. Therefore, positively charged colloidal  $SiO_2-ZrO_2$  can be intercalated into aluminosilicate layers through the ion exchange reaction, producing an intercalation compound  $SiO_2-ZrO_2$ . After calcination, nanosol particles eventually converted into nanometer-sized oxide pillars in the interlayer space of montmorillonite [3,5].

**Characterization:** The chemical compositions of Mt-K10 and SZMK were determined through elemental analysis using

EDX. The main components of the parent mineral (Mt-K10) and catalyst (SZMK) were O, Si, and Al. The Na content of the parent minerals indicates that it was sodium montmorillonite. In SZMK, no sodium was found, but Zr was detected, which indicated that cation exchange had occurred. Using EDX, silica ( $SiO_2$ ) and zirconia ( $ZrO_2$ ) were estimated at a 51.64 and 6.53 mass %, respectively (Fig. 1).

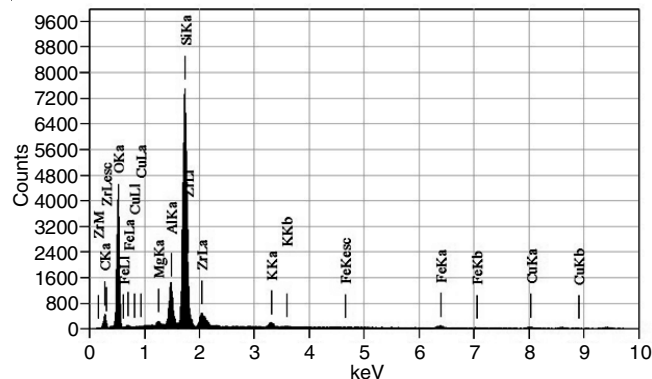


Fig. 1. EDX spectra of SZMK

Fig. 2 shows a series of XRD patterns of Mt-K10 and SZMK after heat treatment. In general, XRD patterns of all the samples were virtually unchanged compared with that of Mt-K10. This indicates sufficient retention of crystallinity during preparation. The diffraction obtained with Mt-K10 peaks at 8.79° (001), 17.71° (003), 19.72° (100), 26.56° (005) and 34.89° (105) corresponding to montmorillonite of hexagonal phase, which was similar to those reported in the literature [3,11]. On calcination at 700 W,  $d_{001}$  slightly increased and shifted to a lower angle. This is because of the small quantity of mixed oxides colloidal particle  $SiO_2/ZrO_2$  still in the Mt-K10 interlayer of SZMK.

TGA/DTA analysis shows a similar results regarding the thermal stability (Fig. 3). The basic structure of Mt-K10 was not reputered by heating, but peak broadening and slight decrease in diffraction intensity were observed. These were closely related to decrease in the crystal size of Mt-K10 due to chemical treatment. Furthermore, stacking disorder among particles may result in XRD peak broadening [12]. The estimated sizes of crystallite Mt-K10 and SZMK (perpendicular to the  $d_{001}$  plane) obtained with Scherrer equation were 34.11 and 21.28 nm, respectively, as reported earlier [13].

TGA/DTA thermograms of Mt-K10 and SZMK after  $NH_3$  adsorption in the region 30-900 °C are shown in Fig. 3. Below 100 °C, a weight loss was due to physisorbed ammonia loss. For Mt-K10, more than 10 % weight loss was observed. However, for SZMK, a weight loss in this temperature region was less than 10 %. Thus, compared to Mt-K10, ammonia was adsorbed more strongly to SZMK acid sites, which had more and stronger acid sites than Mt-K10 due to Lewis acid sites of Zr metal. Song *et al.* [14] states that thermal desorption at elevated temperatures can remove base molecules adsorbed on the solid surfaces of Brønsted and Lewis acid sites. The desorption temperature depends on the interaction strength between the base and surface acid sites.

Physical changes usually result in the endothermic curves of DTA. For modified montmorillonite, the broad endothermic

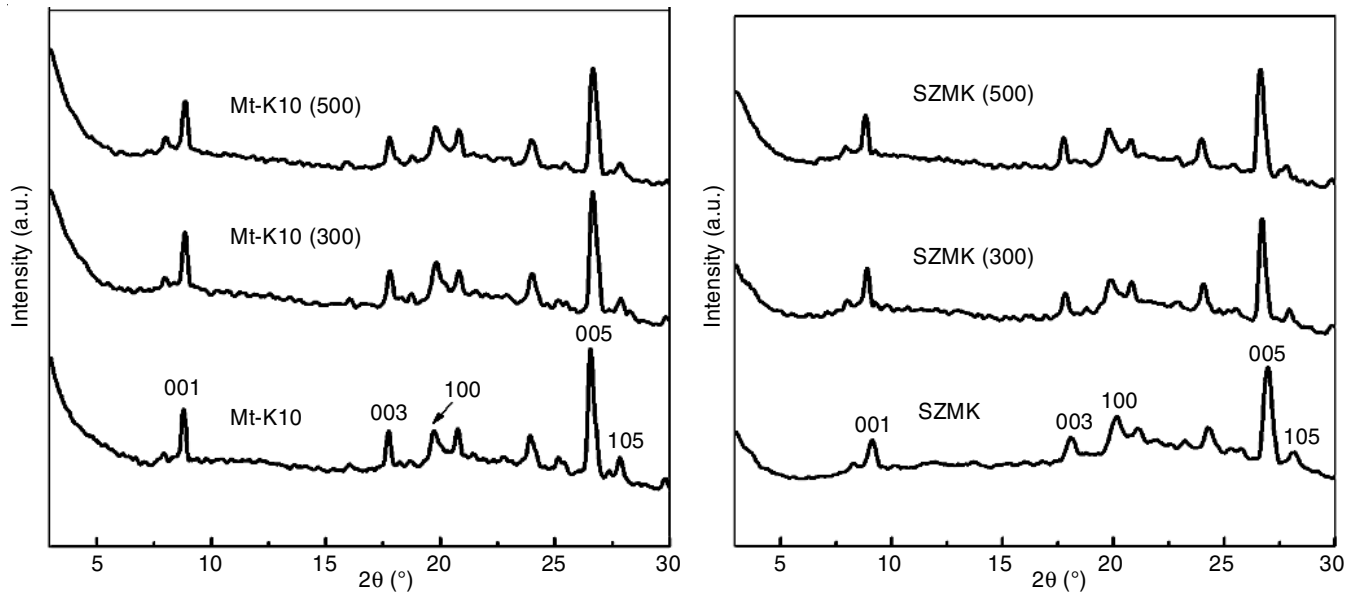


Fig. 2. Diffractogram of Mt-K10 (left) and SZMK (right) before and after heating at 300 and 500 °C

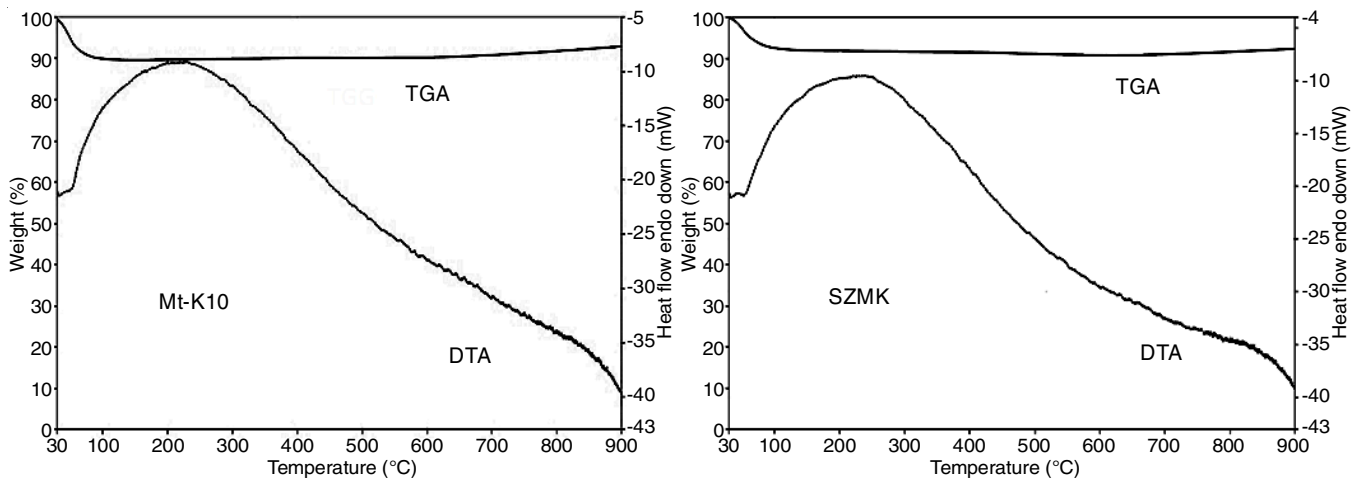


Fig. 3. TGA/DTA curves of Mt-K10 (left) and SZMK (right)

peak between 50 and 450 °C centered at approximately 230 °C, corresponding to the dehydration reaction and acidic proton loss [15]. An area under the DTA peak of Mt-K10 is slightly larger than that of SZMK, which is directly proportional to the heat evolving or flowing into the sample.

For the prepared materials, effect of silica-zirconia on the total surface acidity was measured using ammonia adsorption, which was calculated using the gravimetric method followed by FTIR analysis. Total surface acidity measurements of Mt-K10 and SZMK were 4.83 and 4.99 mmol/g, respectively. In this case, prepared material SZMK with microwave radiation exhibited high total surface acidity.

Fig. 4 presents the FTIR spectra of Mt-K10 and SZMK after treatment with gaseous ammonia. No major differences were observed among the spectra, but they were remarkably different from those obtained before ammonia was adsorbed. The essential peaks among them are absorption peaks at wavenumbers 470, 794, 1056, 1396, 1635, 3441 and 3749  $\text{cm}^{-1}$ . An absorption band at wavenumber 3441  $\text{cm}^{-1}$ , which was identified as -OH stretching vibration of water molecules, indicates that montmorillonite has water absorbing properties. Around

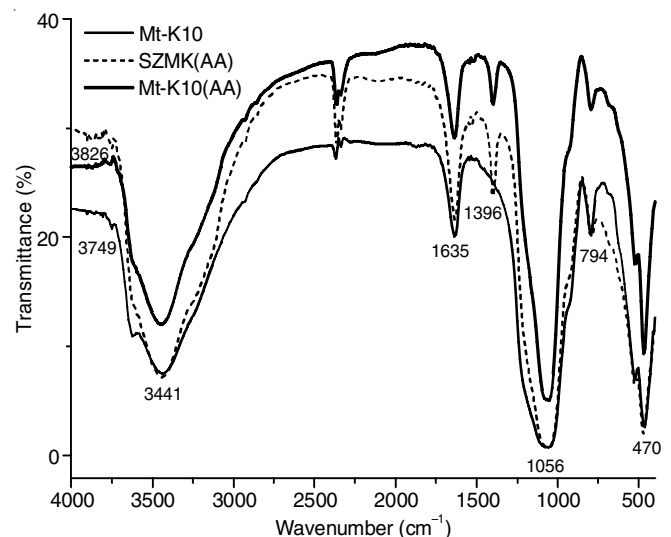


Fig. 4. FTIR Spectra of Mt-K10 and SZMK after adsorbed ammonia

the -OH bending vibration of water molecules, this band was reinforced with an absorption band at 1635  $\text{cm}^{-1}$  [16].

Stretching vibration of the octahedral Al-OH appears at  $3749\text{ cm}^{-1}$  in Mt-K10 and at  $3826\text{ cm}^{-1}$  in SZMK samples. The presence of these bands are attributed to the owing of increasing Si/Al ratio caused by  $\text{SiO}_2/\text{ZrO}_2$  oxide inclusion. Increasing the Si/Al ratio provided a good thermal resistance to pillared montmorillonite [16]. The absorption bands at  $470$  and  $794\text{ cm}^{-1}$  are characteristic of a bending vibration of Si-O-Si. However, an absorption band at  $1056\text{ cm}^{-1}$  is an absorption characteristic of Si-O stretching vibration in the tetrahedral layer. Furthermore, an intense peak at  $1396\text{ cm}^{-1}$  is a characteristic of Brønsted acidity, whereas this peak does not appear on the samples before ammonia adsorption.

Qualitatively, the strength of acid sites can be determined from the absorption peaks in the wavelength range showing the interaction between the catalyst and ammonia. Ammonia adsorption on Mt-K10 and SZMK samples leads to a formation of strongly bound coordinated ammonia, which is evidenced by strong Brønsted acidity. According to Emeis [17], a number of Brønsted or Lewis acid is proportional to a band area of the Brønsted or Lewis peak. A specific area of the peak indicates that an acidity of Brønsted is equal to 42.812 and 52.248 for the Mt-K10 and SZMK, respectively. Thus, SZMK has more acid sites compared with Mt-K10. A mixture of Si-Zr metal oxides in Mt-K10 interlayer contributed to Lewis acid sites. Moreover, these data are reinforced by the results of total acidity. The total acidity increased by  $0.16\text{ mmol/g}$  for SZMK. Using  $\text{N}_2$  gas adsorption analysis, porosity of the parent and modified Mt-K10 was studied. The data are shown in Table-1 and Fig. 5.

Sample	Specific surface area* ( $\text{m}^2\text{ g}^{-1}$ )	Total pore volume** ( $\text{cm}^3\text{ g}^{-1}$ )	Average pore radius** (Å)
Mt-K10	240	2.43	32.92
SZMK	249	2.69	29.32

\*Determined by the multipoint BET method.  
\*\*Determined using BJH pore analysis.

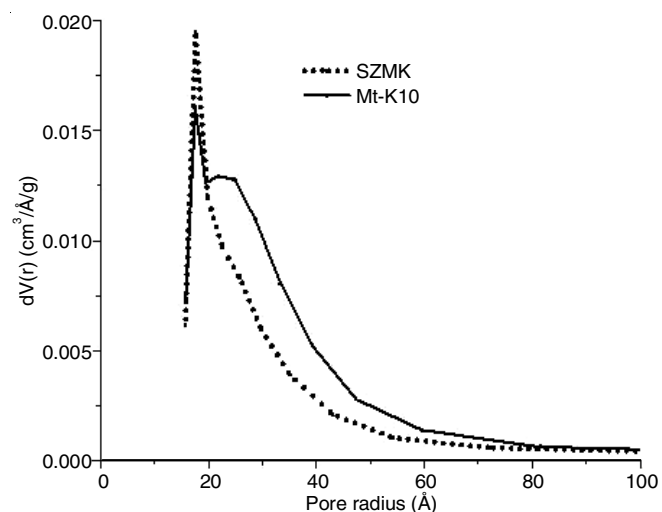


Fig. 5. Pore size distribution of Mt-K10 and SZMK

Nitrogen gas adsorption analysis shows that the specific surface area and the total pore volume of SZMK increased, whereas the average pore radius decreased. Theoretically, calci-

nation process enhances the specific surface area parameter regarding the formation of the metal oxide pillar at the interlayer space of a montmorillonite [18]. The average decrease in pore radius was probably related to the sol-gel mechanism during intercalation. Catalysts with a large specific surface area are preferred because that increases the rate of mass transfer [18], thereby increasing the overall rate of chemical reactions. The small crystallite size (based on XRD data) and the entire pore surface were associated with a large specific surface area.

Fig. 5 shows the pattern of pore size distribution of the samples calculated by the BJH method. The pore size distribution of SZMK was slightly different from that of Mt-K10. This may be due to an increase in the proportion of macropores when Si-Zr is added to the system. SZMK has a narrow size distribution and exhibits mesopores. Moreover, SZMK adsorbed more  $\text{N}_2$  gas than Mt-K10 did due to its higher total pore volume.

**Catalytic activity:** Lauric acid was esterified with methanol by using the catalysts Mt-K10 and SZMK to test their catalytic activity. Furthermore, an experiment was conducted without using a catalyst (blank reaction) for comparison. Di Serio *et al.* [19] proposed a methyl ester formation step through an esterification reaction by using solid acid catalysts. Here, a carbonyl group of lauric acid adsorbs on the Lewis acid site, and methanol adsorbs on the basic site of the catalyst to produce carbocation (step-1). Then, on the catalyst surface, a nucleophilic-attacked carbocation occurs at each methanol hydroxyl group (step 2). The nucleophilic attack generates a tetrahedral intermediate. Finally (step-3), the final product (methyl laurate) was obtained through the desorption of the hydroxyl group from the catalyst surface after breaking the -OH bond, whereas deprotonated catalyst regenerated active species for initiating another catalytic cycle. After the catalytic cycle was completed,  $\text{H}_2\text{O}$  was obtained as a product of esterification.

The conversion of lauric acid into methyl laurate using the parent and modified Mt-K10 catalysts was investigated using GC. The total conversion and product yield were determined based on a reaction chromatogram calculated as follows:

$$\text{Total conversion (\%)} = \frac{[\text{Lauric acid}]_0 - [\text{Lauric acid}]_{\text{product}}}{[\text{Lauric acid}]_0} \times 100$$

$$\text{Methyl laurate (ML) yield (\%)} = \frac{\%[\text{ML}] \times \text{Weight of product}}{\text{Weight of lauric acid}} \times 100$$

Here,  $[\text{lauric acid}]_0$  and  $[\text{lauric acid}]_{\text{product}}$  are lauric acid concentrations in unreacted and final products, respectively. The weight of lauric acid is the same as the initial weight of the reactant. The chromatogram of lauric acid esterification using modified Mt-K10 catalyst (SZMK) showed that almost all the lauric acid was converted into methyl laurate (Fig. 6). Thus, the esterification reaction completed successfully.

Under the conditions applied in this study for the conversion of lauric acid to methyl laurate (Fig. 7), all materials have catalytic activity. A similar behaviour was reported by Zatta *et al.* [20] while developing phosphoric acid-activated clays. In this case, acid concentration and treatment time were limited to develop the best catalyst for lauric acid esterification with methanol. Present results showed that the catalyzed esterification reaction produced large conversion and product yields compared with that obtained in the reaction without a catalyst. Further-

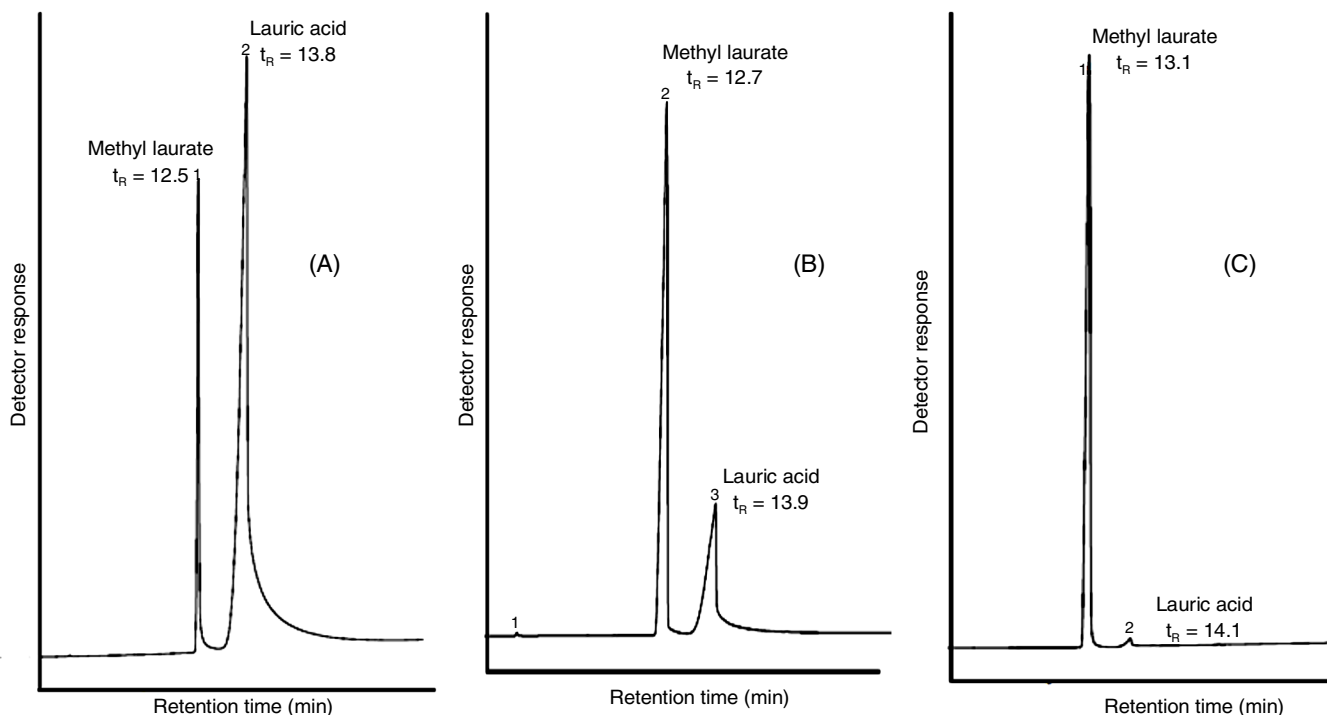


Fig. 6. Chromatogram of product esterification of lauric acid using no catalyst (blank) (A), catalyst Mt-K10 (B) and SZMK (C)

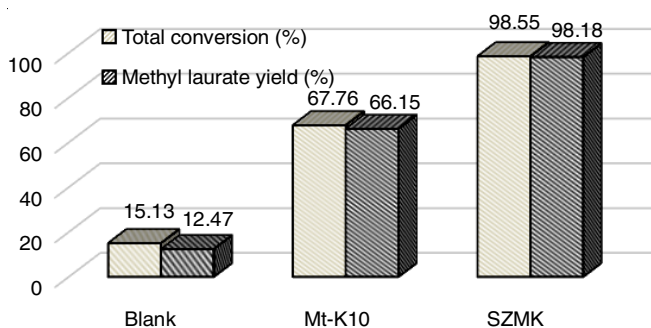


Fig. 7. Total conversion and methyl laurate yield of the catalysts in the esterification reaction

more, esterification with a mixture of Si-Zr metal oxide calcined by microwave radiation using a modified Mt-K10 catalyst provides higher results than that obtained using montmorillonite K10 (Mt-K10).

FTIR data supports the differences in these results (Fig. 7). It quantitatively showed that Brønsted acid sites indicated by the peak at  $1396\text{ cm}^{-1}$  (Fig. 4) have the intensity 23.778, which is less than the absorption intensity of Mt-K10 by 32.203. According to Banwell and Mccash [21], more polar the bond, greater will be the absorption intensity. The decrease in the absorption intensity of the functional groups of SZMK was due to reduced polarity of the bonds between its atoms. The polarity of SZMK is lesser than that of methanol. Consequently, in reaction, methanol will minimize the interactions with the pore walls of SZMK, increasing the diffusion rate of active sites. This allows to speed up the esterification reaction. Moreover, a large surface area of SZMK (Table-1) provided positive catalytic properties to SZMK itself. The high specific surface area tends to strongly adsorb the reactants and hinder the adsorption-desorption mechanism of reactants and products.

**Catalyst recovery and reusability:** The recovery and reusability of the catalytic material, silica-zirconia/Mt-K10, were examined. The catalyst was separated, washed with *n*-hexane, dried at room temperature, and exposed to microwave radiation energy of 200 W for 10 min prior to the catalytic run. The catalyst reusability in the esterification reaction of lauric acid with methanol was examined for two cycles with inconsistent activity and the results are presented in Fig. 8. The catalytic activity decreased by 15 % on an average due to the leaching of Lewis or Brønsted acid sites during the esterification process.

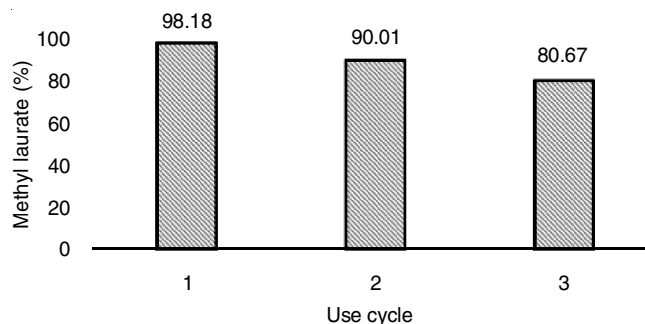


Fig. 8. Use cycle of the SZMK catalyst in the esterification reaction

## Conclusion

Present research shows that the chemically modifying montmorillonite K10 (Mt-K10) using a mixed silica-zirconia increases the acidity, porosity and thermal stability of the total surface. Silica-zirconia/Mt-K10 potentially improves the catalytic activity of lauric acid. Lauric acid can be converted to methyl laurate by using catalysts exclusively containing Lewis or strong Brønsted acid sites.

### ACKNOWLEDGEMENTS

The authors are grateful to Kemenristek Dikti Indonesia for financial assistance through the BPPDN scheme.

### CONFLICT OF INTEREST

The authors declare that there is no conflict of interests regarding the publication of this article.

### REFERENCES

1. Y.S. Han, H. Matsumoto and S. Yamanaka, *Chem. Mater.*, **9**, 2013 (1997); <https://doi.org/10.1021/cm970200i>
2. S.J. Sekewael, K. Wijaya, Triyono and A. Budiman, *Int. J. ChemTech Res.*, **10**, 62 (2017).
3. Y.S. Han and S. Yamanaka, *J. Solid State Chem.*, **179**, 1146 (2006); <https://doi.org/10.1016/j.jssc.2006.01.013>
4. S.J. Sekewael, K. Wijaya, Triyono and A. Budiman, *Asian J. Chem.*, **28**, 2325 (2016); <https://doi.org/10.14233/ajchem.2016.19982>
5. J.H. Choy, J.B. Yoon, H. Jung and J.H. Park, *J. Mater. Chem.*, **13**, 557 (2003); <https://doi.org/10.1039/b208929g>
6. Y. Kameshima, T. Koike, T. Isobe, A. Nakajima and K. Okada, *Mater. Res. Bull.*, **44**, 1906 (2009); <https://doi.org/10.1016/j.materresbull.2009.05.005>
7. Ruslan, K. Wijaya and Triyono, *Int. J. Appl. Chem.*, **9**, 15 (2013).
8. R. Fazaeli and H. Aliyan, *Appl. Catal. A Gen.*, **331**, 78 (2007); <https://doi.org/10.1016/j.apcata.2007.07.030>
9. R.D. Aher, M.H. Gade, R.S. Reddy and A. Sudalai, *Indian J. Chem.*, **51A**, 1325 (2012).
10. M. Ayoub and A.Z. Abdullah, *Catal. Commun.*, **34**, 22 (2013); <https://doi.org/10.1016/j.catcom.2013.01.007>
11. A. Ghebaur, S.A. Gărea and H. Iovu, *U.P.B. Sci. Bull.*, **73B**, 169 (2011).
12. J.P. Kumar, P.V.R.K. Ramacharyulu, G.K. Prasad and B. Singh, *Appl. Clay Sci.*, **116-117**, 263 (2015); <https://doi.org/10.1016/j.clay.2015.04.007>
13. S.J. Sekewael, K. Wijaya and Triyono, *Indones. J. Chem. Res.*, **6**, 38 (2018). <https://doi.org/10.30598/ijcr.2018.6-sjs>
14. C. Song, W.C. Lai, A.D. Schmitz and K.M. Reddy, Characterization of Acidic Properties of Microporous and Mesoporous Zeolite Catalysts using TGA and DSC, ACS Division of Fuel Chemistry, Preprints, **41**, pp. 71-76 (1996).
15. B. Li, Z. Liu, C. Han, W. Ma and S. Zhao, *J. Colloid Interface Sci.*, **377**, 334 (2012); <https://doi.org/10.1016/j.jcis.2012.03.067>
16. P. Yuan, F. Annabi-Bergaya, Q. Tao, M. Fan, Z. Liu, J. Zhu, H. He and T. Chen, *J. Colloid Interface Sci.*, **324**, 142 (2008); <https://doi.org/10.1016/j.jcis.2008.04.076>
17. C.A. Emeis, *J. Catal.*, **141**, 347 (1993); <https://doi.org/10.1006/jcat.1993.1145>
18. A. Gil, S.A. Korili, R. Trujilano and M.A. Vincente, Pillared Clays and Related Catalyst, Springer Science+Business Media: New York (2010).
19. M. Di Serio, R. Tesser, L. Pengmei and E. Santacesaria, *Energy Fuels*, **22**, 207 (2008); <https://doi.org/10.1021/ef700250g>
20. L. Zatta, L.P. Ramos and F. Wypych, *Appl. Clay Sci.*, **80-81**, 236 (2013); <https://doi.org/10.1016/j.clay.2013.04.009>
21. C.N. Banwell and E.M. Mccash, *Fundamental of Molecular Spectroscopy*, McGraw-Hill College, USA (1994).